A New Parallel Fold Construction Method from Borehole Dip for Structural Delineation*

Tetsushi Yamada[1], Isabelle Le Nir[2], Eric Moscardi[3], and Arnaud Etchecopar[4]

Search and Discovery Article #41969 (2016)**
Posted December 26, 2016

*Adapted from extended abstract prepared in conjunction with oral presentation given at AAPG 2016 Annual Convention and Exhibition, Calgary, Alberta, Canada, June 19-22, 2016

[1]Schlumberger, Clamart, Ile-de-France, France (TYamada@slb.com)
[2]Schlumberger, Clamart, Ile-de-France, France
[3]Schlumberger, Grabels, Midi-Pyrénées-Languedoc-Roussillon, France
[4]Consultant, La Rochelle, Aquitaine-Limousin-Poitou-Charentes, France.

Abstract

Dips derived from borehole images are used to create high quality structural models in the vicinity of boreholes using an existing workflow based on conventional geological concepts. Such local models significantly improve the estimation of the oil in place and help determine the most effective way to produce it. Another workflow applies the same concepts to dip data from multiple wells in combination with surface seismic data. The main concept of both workflows is the similarity of the layers during deformation. Although this is robust whatever the deformation type (e.g. fold, drag, rollover), it is not very accurate for folds, yet most oil reservoirs are in the parallel fold domain. Methods for parallel layers construction are much more challenging than the similarity approach. The existing parallel method being not sufficiently stable, we propose a totally new approach. Our method starts by delineating structures along the well using a new automatic stereonet analysis applied to dips selected by an interpreter. This technique helps the interpreter identify the structure type (i.e. zones with same structural axis) at different scales. Based on this delineation, the interpreter selects for each structure a type from monocline, drag folds (normal/reverse), rollover, and similar/parallel fold. The corresponding cross section is automatically displayed. A major improvement to previous approaches has been made in the parallel fold model. The new method is not only very accurate but also very robust. Results are no longer disturbed by erratic dips. The computed geological layers are first displayed on a cross section perpendicular to the structural axis. Once validated by the interpreter they can be displayed on a curtain section or as three-dimensional surfaces. Case studies demonstrate that the new technique to reconstruct parallel folds greatly improves the accuracy of the reservoir geometry. The workflow enables interpreters to run different scenarios when several structural types are considered. Local structural information such as surfaces and the structural axis can be further used to constrain three-dimensional reservoir models built from multiple wells and seismic, facilitating well placement decisions and reserve evaluation.

Introduction

One of the main applications of borehole image data is near-well structural analysis from borehole dips to create geological cross sections. Geologists use this analysis to better understand the geometry of geological structures in the vicinity of the well, and it complements the structural description from seismic data. However, obtaining seismic data is costly and acquiring a good-quality seismic section is often difficult when layer boundaries dip steeply, for example, at the limb of folds or around salt bodies. Near-well structural interpretation can be initiated using only borehole dips from a single well. This interpretation, however, requires considerable expertise as well as knowledge of the local geology. In addition, manually drawing geological cross sections is time-consuming work. Etchecopar and Bonnetain (1992) introduced a workflow and computer methods to facilitate the analysis and automate cross-section construction while respecting the orientation of dips in agreement with the basic rules of structural geology. The application draws geological cross sections almost instantly, allowing interpreters to test different geological scenarios. Sedimentary structures such as cross bedding can also be drawn to analyze depositional environments. Marza et al. (2014) extended this concept and modeled geological structures with 3D visualization and incorporating data from multiple wells.

In the past few decades, there have been major advances in borehole image data acquisition and processing techniques both for wireline logging and logging while drilling (LWD). On the wireline side, the dipmeter tools with a few electrodes embedded were replaced by borehole imagers with increased azimuthal coverage resulting from more embedded electrodes. Today, imagers can acquire high-resolution data in both water- and oil-based mud conditions. The vertical and horizontal sampling rates of standard wireline microresistivity tools are 2.54 mm (0.1 in.) and the resolution (focusing zone) is 5.08 mm (0.2 in.). The quality and the resolution of LWD imagers have also been considerably improved (vertical/horizontal resolution is up to 0.4 in). Other types of imaging tools such as ultrasonic and density also enable the interpretation of major bed boundaries and faults. On borehole images the important structural (e.g., bedding, faults, unconformities) and sedimentary (e.g., cross bedding, basal conglomerates) features are clearly recognized. This allows interpreters to limit the possible geological scenarios, increasing the confidence and accuracy of the interpretation and reservoir description. Advanced techniques have been introduced to automate dip detection and classification on borehole images (e.g., Kherroubi and Maeso, 2016; Ye, 2015; Antoine and Delhomme, 1993). Near-well structural analysis has progressed to become much more accessible and the processing time has been greatly shortened.

The existing structural analysis techniques can be used with the modern imagers. A key drawback, however, is the method to construct cross sections with parallel layers (i.e., layers with constant thickness). The accuracy of the geometry of the deformed structure, such as folds creating oil traps, is critical for better reservoir description, and the parallel approach is often appropriate at the regional and basin scale. Although the method works well in simple cases, it is not sufficiently robust with real data. For this reason, we have developed another method to replace the existing parallel model with a totally new approach, which has been implemented in an application that enables the geologist to run the whole structural analysis workflow. The purpose of this paper is to present the parallel structures computed with our new application and to show how the results improve understanding of the reservoir geometry. It also introduces some new techniques in the structural analysis workflow. The geological cross sections are computed on a 2D cross section, but they can be extended to a 3D model for visualization and 3D horizon construction.

Workflow of Structural Interpretation from Borehole Dips

Borehole dips Analysis Tools

In the structural interpretation workflow, geologists make decisions at different stages using all available data, but mainly based on borehole dips. The main decisions concern defining the limits of structures, stratigraphic polarity, and selecting structural models. For this type of analysis the appropriate tools for the visualization of dips are indispensable. A borehole dip is essentially a plane intersecting the well path. Given the well trajectory, it can be defined with three independent properties: measured depth, dip inclination (magnitude), and dip azimuth. As there are three parameters, several ways of visualizing them on a 2D screen are possible. The arrow plot (aka tadpole plot, Figure 1b) is a conventional plot containing all three properties. The theoretical patterns of the arrow plot for different geological structures are presented in several books or articles (e.g., Schlumberger, 1970), but most geologists are not familiar with interpreting the structure based on this plot. Geologists are more familiar with the interpretation of the pattern of poles of dips on the stereonet plot (Figure 1c). Although it does not contain depth information, interpreters can analyze the data from specific depth intervals. The plot shows a concentration or alignment on a great circle when the data are from the same structure. The dip vector plot (Figure 1d) is also a recommended plot, which is drawn by creating unit vectors of dip azimuth or inclination and connecting them in the order of the measured depth. The vectors are generally colored as a function of the measured depth. This plot helps interpreters find the structural breaks and also indicates the structure type. Each plot has its own advantages for highlighting specific characteristics of the structure, and interpreters should analyze dips by using several plots for a comprehensive analysis of the structure. Although this analysis largely limits the possible geological scenarios, more than one interpretation is sometimes possible and interpreters must refer to the geological context of the region.

Workflow

The structural analysis workflow is shown in Figure 2. The mandatory inputs are the dips representing bed boundaries along the borehole trajectory, but other inputs can be used as additional information, such as major recognized faults or unconformities. Filtering out the dips that do not follow the global trend is an important first step, because dips detected automatically, or even delineated manually, generally contain perturbed dips that are not consistent with the regional geological structure. The remaining dips are considered the structural dip; they are the dips consistent with the structure at the regional scale. It is also possible to extract structural dips by analyzing dips from sedimentary structure using the method proposed in Etchecopar and Dubas (1992).

The main workflow consists of two steps: automatic structural analysis and cross-section computation. The first step is an automatic and interactive structural analysis. In this step, interpreters can refine zone(s) of the same structural unit along the well trajectory. A structural unit is a set of layers to which the same deformation and/or tilting was applied. Without a priori knowledge, we do not know how many structural units a well penetrates. A key indicator for the zone definition is the pattern of poles on the stereonet. There are two patterns based on geological principles: green pattern and orange pattern. The green pattern is a concentrated distribution, and is observed when the structure is not deformed (e.g., monocline). The green pattern is characterized by the mean dip and also the strike of the mean dip (called the pseudo-structural axis). The orange pattern is an elongated distribution along a great circle (cylindrical structure) or a small circle (conical structure), and it is observed when the structure is deformed (e.g., fold, fault with drags). The orange pattern is characterized by the structural axis that

corresponds to the pole of the plane of the great or small circle and also conicity if conical structure. Etchecopar and Dubas (1992) proposed an automatic zonation method from dips by differentiating green and orange patterns. This method starts by grouping consecutive dips with thresholds and combines the groups if they are considered to belong to the same structural unit by checking the pattern of dips on the stereonet. The zones must be verified and refined by the interpreter by analyzing dips on several plotting tools and by using available external data, such as major faults and unconformities observed on the borehole image and lithology logs (e.g., gamma ray). At the same time the geologist must define the stratigraphic polarity for each dip (normal or reverse, as this affects the resulting cross section), and estimate the possible geological structure based on the structural type in preparation for the next step.

A difficulty in defining zones is the scale dependency of the structure. For example, a monocline structure at a small scale might be part of the limb of a fold at a larger scale. Figure 3 shows a new way to visualize the structure type as a function of the scale. The x-axis is the length of the scale and the y-axis is the measured depth. The red-orange color shows the orange pattern, and the blue-green color is the green pattern. To create this matrix, a test of the orange patterns is successively conducted with the dips in a sliding window along the measured depth. If no orange pattern is detected, the program checks if the dips show a green pattern. The color density shows the quality of fit represented by the fitting error.

Once the structural zones are set, a selected geological model is applied to each structural zone to construct the cross sections. Before applying a model, further processing of the dips is often necessary; smoothing should be applied to further eliminate erratic dips, and resampling should be applied when structural dips are poorly sampled. Several geological scenarios can be analyzed by applying different models and modifying the structural zones. Once the computed cross section is validated, the display of the structure can be highlighted with a lithology log.

Existing Models

The two geometric models for constructing geological layers respect different assumptions in the geometry of layers: similarity and parallelism. Both models build layer geometries by translating dips in the direction along a specific plane, the translation plane, in 2D. In the similar model, the translation plane is common to all the dips, whereas in the parallel model it is unique to each dip and defined as a plane orthogonal to the dip plane. The computation step is shown in Figure 4 using an example of the parallel model. Dips and the translation plane are first projected on a 2D plane, representing the dips with sticks and the translation plane with a translation axis. Layer lines are created using only the angles of the dip sticks. A layer line at the nth dip is successively extended by firstly translating dip sticks one after another in their translation directions and then linking them at their intersection. The position of the translating stick is constrained by the previous neighboring stick; i.e., the translated one and the previous one must be at the same distance from the intersection of their extended lines. The computed layer line for the nth dip is a polyline (i.e., continuous line composed of line segments) made with intersections of the nth dip and the $N-1$ translated dips, where N is the number of input dips.

Using a common translation plane for all the dips results in layers with the same thickness in the direction of the translation axis and identical geometries in the layers. This corresponds to the definition of the geometry of a similar fold, for which the layer thickness is constant in the direction of the axial plane (Figure 5a). In the similar fold model the translation plane must be selected so that it corresponds to the axial plane,

which goes through the middle of the elongated cloud of poles on stereonet. This method is applicable to faults with drag and to rollover and monocline structures by assuming that they are similar structures or part of a similar structure. The translation planes are defined as the fault plane, the detachment plane, and the plane containing the pole of the mean dip, respectively. On the other hand, the parallel model preserves the layer thickness measured perpendicularly to the initial dips, which corresponds to the layer thickness before folding (Figure 5b). This corresponds to the definition of the parallel fold. The instability of the parallel model was due to the translation axes crossing each other inside the hinge zone of the folds.

New Parallel Model (Cobweb Method)

The newly incorporated parallel model uses the kink method proposed by Suppe (1985), extending the concept to borehole dips. Because this method is not restricted to kink folds, we prefer to call it the cobweb method. Consider a typical spider web of the spiral orb web. It is known that spiders first create radials (warp threads) and methodically add a spiral (weft thread) using the radials as guidelines. Strictly speaking, the web is not made of concentric circles but is a spiral, although it looks like the geometry of a concentric fold for which the layer thickness is parallel. The cross section must be created on a 2D plane that preserves the true thickness and represents the structure. In the case of the orange pattern, the plane perpendicular to the structural axis is the plane on which the structural cross section must be constructed. In the case of a green pattern it is the plane perpendicular to the pseudo-structural axis. The stratigraphic polarity of dips is also taken into account.

The cobweb method consists of two steps: the construction of warp threads (guide web) and dip propagation using the warp threads. In the first step, a guiding web is created from the dips on the well trajectory. The initial webs are the bisectors of perpendiculars of adjacent dips located at the middle of the dips (Figure 6b). To extend the layers maximally by using the input data in the following step, the perpendiculars of the top and bottom dips are added in the initial web set. The number of initial threads corresponds to the number of initial dips plus one. The warp web is created by iteratively merging the threads, starting from the initial set of threads as follows:

Step 1: Search all the intersections (I_1, I_2, I_3,…, I_{N+1}) of adjacent threads in the current set of threads (T_1, T_2, T_3,…, T_N) (Figure 6c)
Step 2: Find the intersection I_n of (T_n, T_{n+1}) with the shortest distance from the well (the circled intersection in Figure 6c)
Step 3: Stop the threads (T_n, T_{n+1}) at the intersection and continue with a new thread T_{new} (Figure 6d)
Step 4: Update the thread set by removing (T_n, T_{n+1}) and adding T_{new}

The direction of the new thread is defined as the bisector of the perpendicular to the dips just above T_n and just below T_{n+1} (n is ordered from top to bottom). The iteration ends when no more intersections are found or if there is only one thread in the set (Figure 6g). The warp threads delimit the 2D plane into several areas and each area contains one dip.

In the second step, the input dips are extended in their area. When they reach the limit of their area, the lines continue but use the dip angle of the next area (Figure 6h). The outside of the hinge zone shows the same geometry as the previous method but the inside of the hinge zone is also properly reconstructed thanks to the merged guiding threads. This method is very effective for constructing parallel layers including a parallel fold in a vertical well and a monocline structure in a horizontal well. The method does not work when the input dips are nearly

perpendicular to the well trajectory because the guiding web becomes very narrow and dips cannot be propagated away from the well. The gradual change of dips leads to a smoother geometry at the hinge zone of the fold.

The method was applied to the dips for two imaginary wells from a photograph of a carbonate outcrop near Montpellier, France (Figure 7). The entire structure is folded with anticlines and synclines of different wavelengths and the layer thickness is preserved. The dips show an orange pattern on the stereonet. The middle part is an anticline fold with a smaller curvature than the others. The right side of the structure extends relatively horizontally. Well V is drilled vertically from the right side of the limb of the fold in the middle to the other side. Well H is drilled horizontally going through the fold axes. In both cases the layers are successfully constructed. The extension of the drawing is limited by the geometry: in well V the dips are propagated sufficiently to the left side because the angle between the perpendicular of the bottom dip and the well is relatively large whereas the right side is not because the corresponding angle of the top dip is small. In well H a good volume of the structure can be reconstructed.

3D Model and Other Projections

As mentioned previously, the cross section is computed on the plane perpendicular to the structural axis (orange pattern) or pseudo-structural axis (green pattern). Assuming that the structure is continuous in the direction perpendicular to the cross-section plane, the 3D model can simply be created by translating the nodes composing the layer lines on the 2D cross section along an axis (translation axis). The translation axis of a cylindrical structure and a monocline structure correspond to the structural axis and the pseudo-structural axis, respectively, and they are common to all the nodes. For conical structures the translation axis deviates relative to the structural axis by an angle that is equal to the difference between 90° and the degree of conicity. Given this information, the orientation of the tangent line is computed by rotating the pole around the structural axis by 90° (Figure 8). The translation axis corresponds to the outer product of the pole and the tangent line. This method can be generalized for cylindrical structures that have a conicity of 90°. Figure 9 shows the near-well 3D model of the structure computed for well H in Figure 7 and its map view. We assumed that the well is in the direction of the azimuth of 40°. The structural axis is perpendicular to the computed cross section (i.e., dipping by an angle of 20° toward the 310° azimuth). The offset of projection is set to 50 m. To display the cross section on a given plane (i.e., not perpendicular to the structural axis) it is sufficient to compute the intersections of the 3D surfaces and the plane. The curtain section is a vertical section containing the well trajectory, and it is approximated by a set of vertical planes. The computed cross section can also be projected on the curtain section by searching the intersections between the 3D surfaces and the vertical planes.

Example with Well Data

The workflow was applied to two lateral wells drilled in shale formations. In this abstract, we assume that there are no faults for simplicity and as a time constraint, but this should be analyzed further for a more detailed interpretation. The first example is a simple monocline structure (Figure 10). The mean dip is 7.4° toward an azimuth of 295.8°, indicating a slight tilting. The pseudo-structural axis is in N25.8°. The well was drilled almost in the north direction. Figure 10 shows the cross section with several angles and the 3D representation of the surfaces. The second case is the well drilled in the Marcellus Formation in Pennsylvania (Figure 11) almost consistently in the azimuth at about 342°. The

dip shows an orange pattern indicating a fold structure. The structural axis is almost horizontal, directed 247.3°. Although it is difficult to imagine from dips, the computed structures show the geometry of the structure and the relative position of the well in the structure.

Conclusions

We described a structural analysis workflow from borehole dips incorporating a new method for creating parallel layers. Based on the interpreted dips, the cross-section construction is quick and robust and gives the geologist a tool to evaluate and visualize the geological structure and its geometrical relation to the well trajectory. The computed cross section and the 3D display can reveal details of the structure geometry away from the trajectory that cannot always be visualized with seismic data. Local structural information such as surfaces and the structural axis can be further used to constrain 3D reservoir models built from multiple wells and seismic, facilitating well placement decisions and reserve evaluation. In some cases, however, manual modifications of the layer geometry by interpreters might be necessary because of a change of layer thickness due to sedimentation. The analysis can be initiated with a single-well data set, but combining multiple well data sets is recommended to reduce uncertainty. Although borehole image logs are commonly acquired, they are not always used for further structural analysis. The workflow and new method make it possible to systematically conduct structural analysis in a standard interpretation workflow in order to optimize the use of data resources.

Acknowledgments

The authors thank Schlumberger for permission to publish this work. We would also like to thank our colleagues for their support, especially Randy Koepsell, Mi Zhou, Stephen D. Sturm, and Weixin Xu.

References Cited

Antoine, J.N, and J.P. Delhomme, 1993, Method to Derive Dips from Bedding Boundaries in Borehole Images: SPE Formation Evaluation, SPE-20540-PA, p. 96-102.

Etchecopar, A., and J.L. Bonnetain, 1992, Cross Sections from Dipmeter Data: American Association of Petroleum Geologists Bulletin, v. 76/5, p. 621-637.

Etchecopar, A., and M.O. Dubas, 1992, Methods for Geological Interpretation of Dips: SPWLA 33rd Annual Logging Symposium, 14-17 June 1992, Oklahoma City, Oklahoma, 21 p.

Kherroubi, J., and C. Maeso, 2016, Lamination Analysis from Electrical Borehole Images: A Quantitative Workflow: SPWLA 57th Annual Logging Symposium, 25-29 June 2016, Reykjavik, Iceland, 16 p.

Marza, P., L.I. Trøan, B.A. Bakke, F. Perna, V. de Leeuw, A. Khan, M. Bower, and H. Charef-Khodja, 2014, Accurate Structural Model in Near-Well Space from Borehole Images: EAGE Borehole Geology Workshop, Optimizing the Use of Your Borehole Image Data, 12–15 October 2014, Dubai, United Arab Emirates.

Ramsay, J.G., 1967. Folding and Fracturing of Rocks: McGraw-Hill, New York, 568 p.

Schlumberger, 1970, Fundamentals of Dipmeter Interpretation: Schlumberger, New York, 145 p.

Suppe, J., 1985, Principles of Structural Geology, Prentice-Hall, New Jersey, 537 p.

Ye, S.J., 2015, A Robust Automatic Dip Picking Technique to Improve Geological Interpretation and Post-Drill Formation Evaluation of Azimuthal Wellbore Image Logs: SPE Annual Technical Conference and Exhibition, 28-30 September 2015, Houston, TX, SPE-175026-MS, p. 4355-4371.

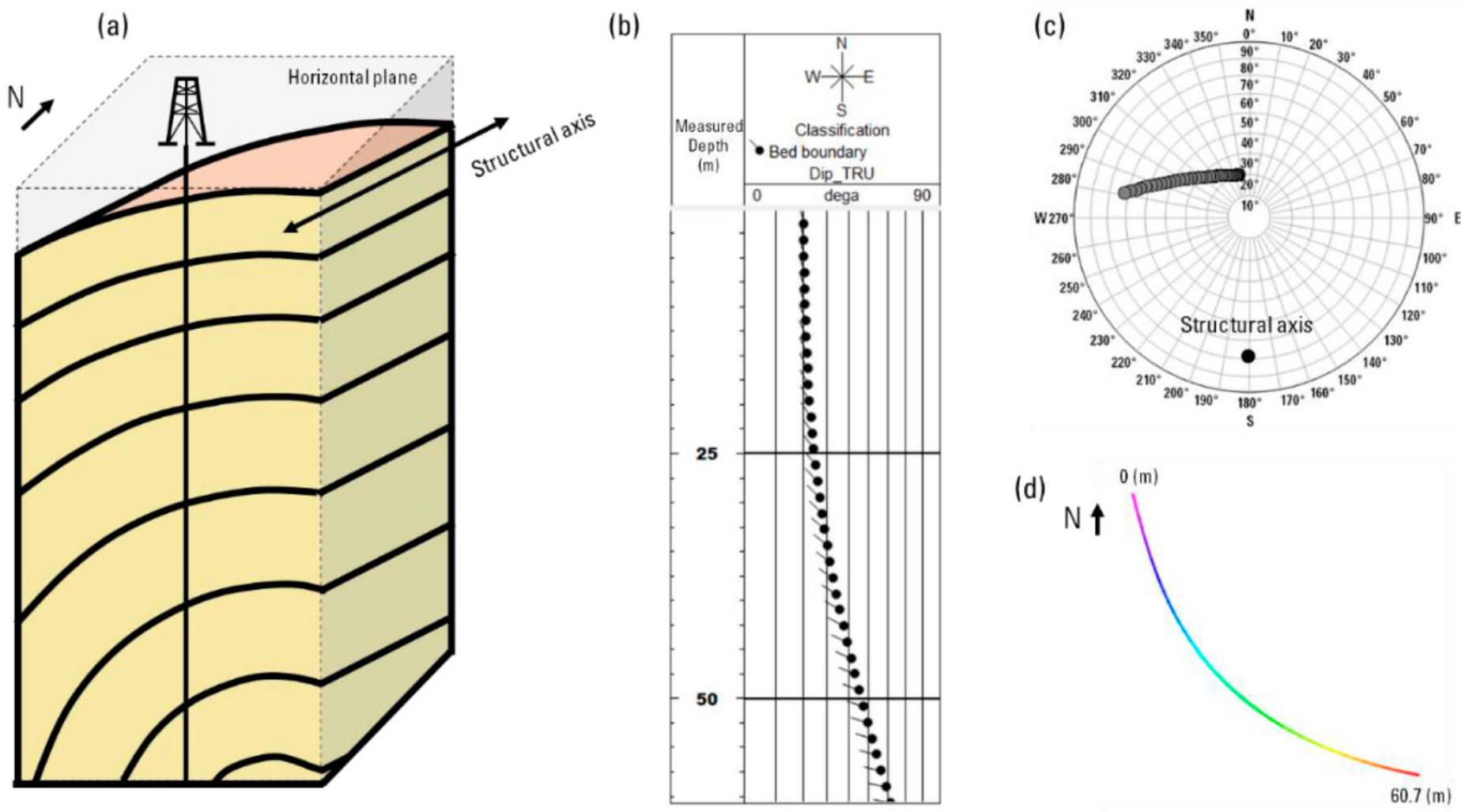

Figure 1. Plots representing the structure of a concentric fold dipping 20° to the north: (a) synthetic cross section, (b) arrow plot, (c) stereonet plot (upper hemisphere, Schmidt net), (d) azimuth vector plot.

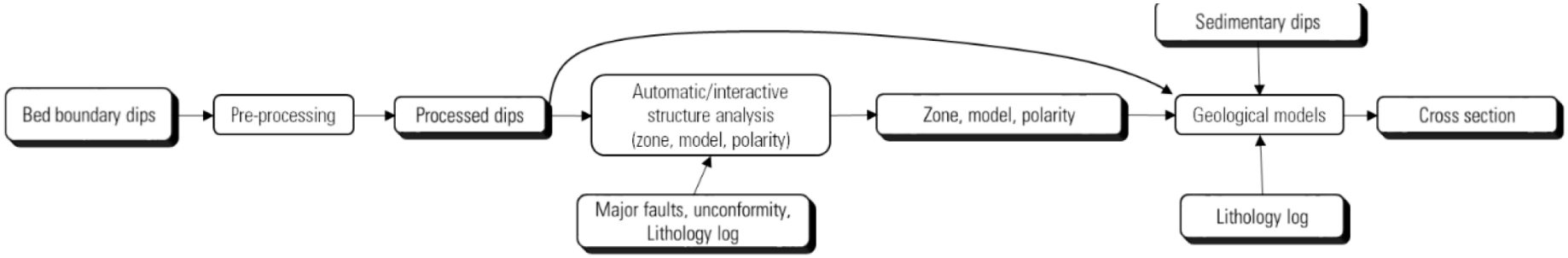

Figure 2. Structural analysis workflow.

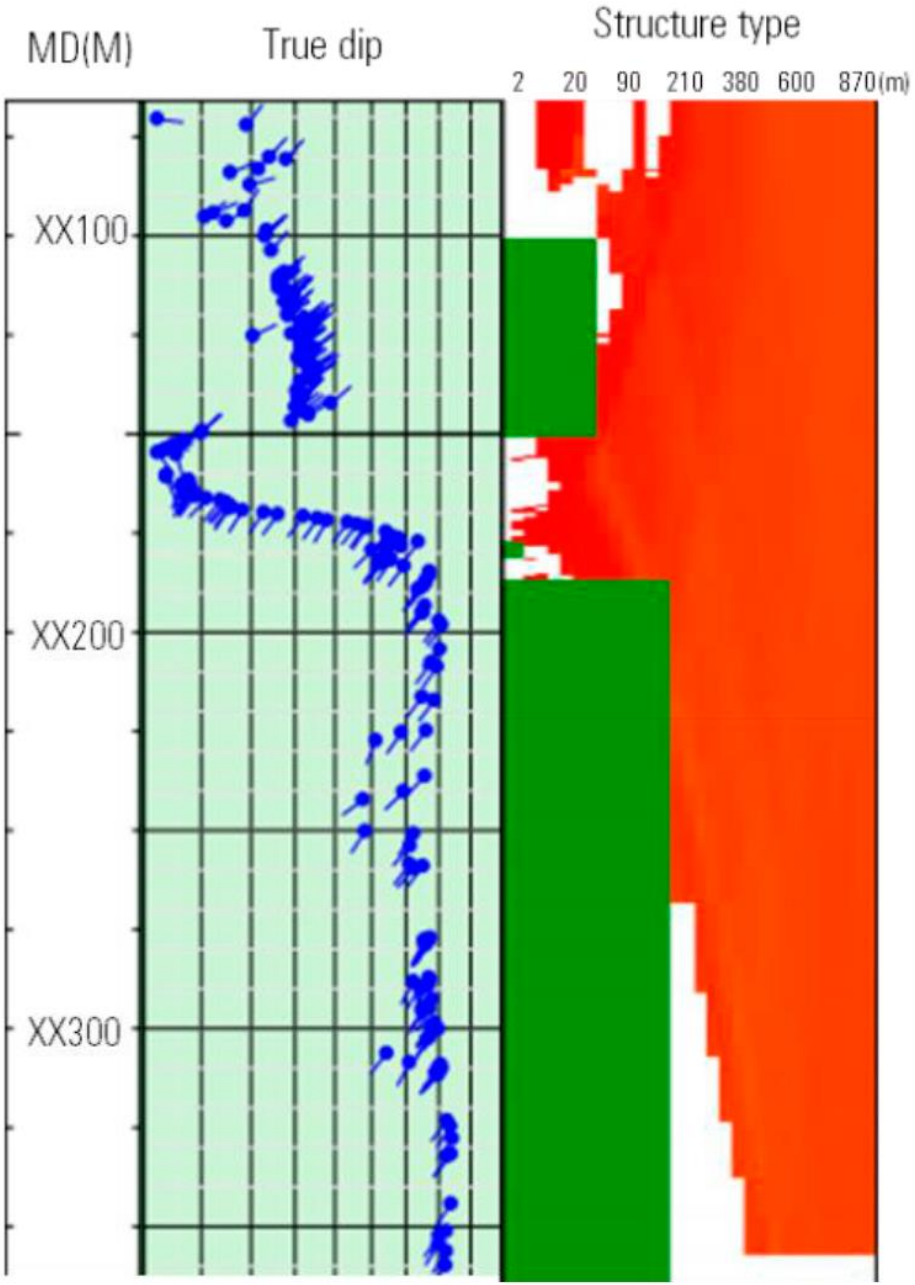

Figure 3. An example of a structure type matrix.

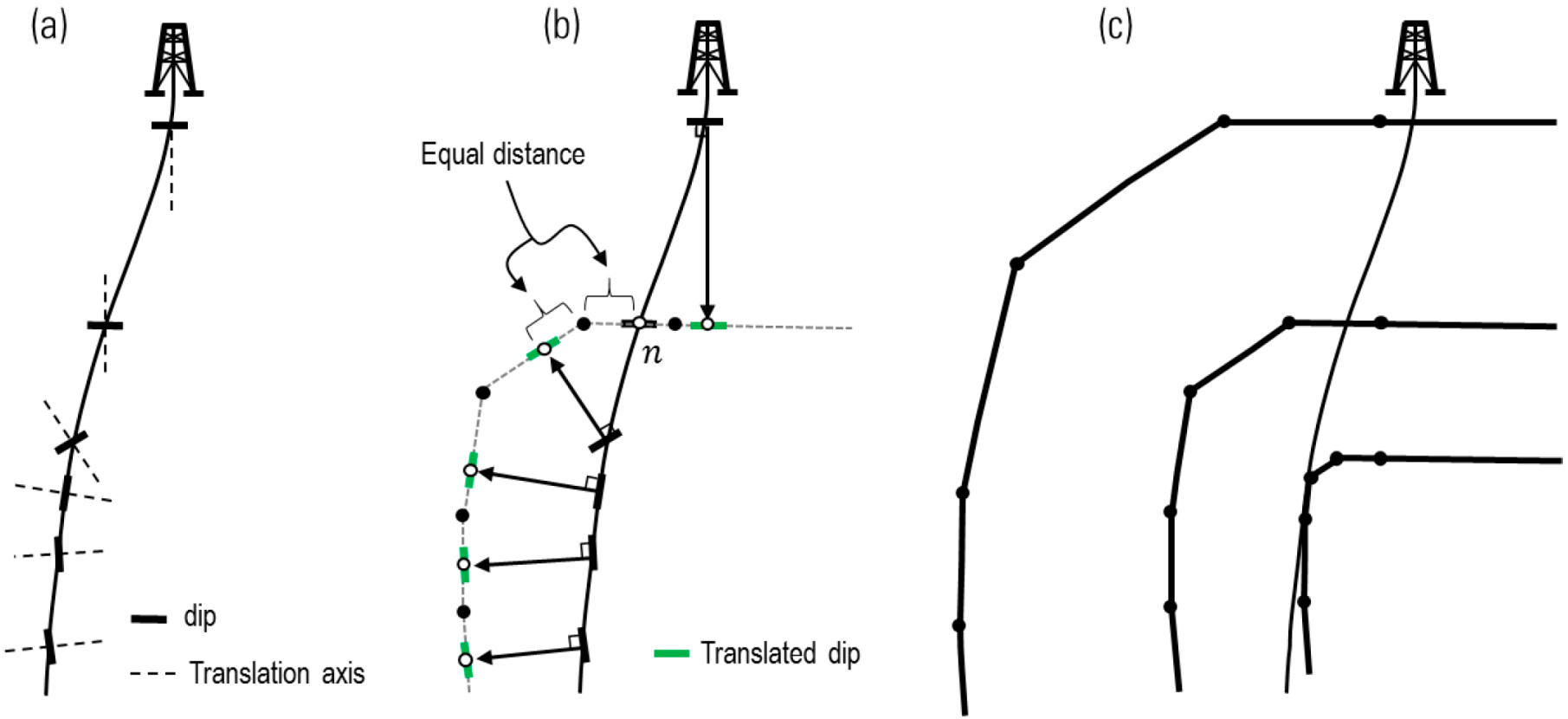

Figure 4. Computation steps of the existing parallel model: (a) input dips projected on a cross section, (b) layer geometry constructed for the second dip from top, (c) geometry of layers computed for the first, second, and fourth dips from the top.

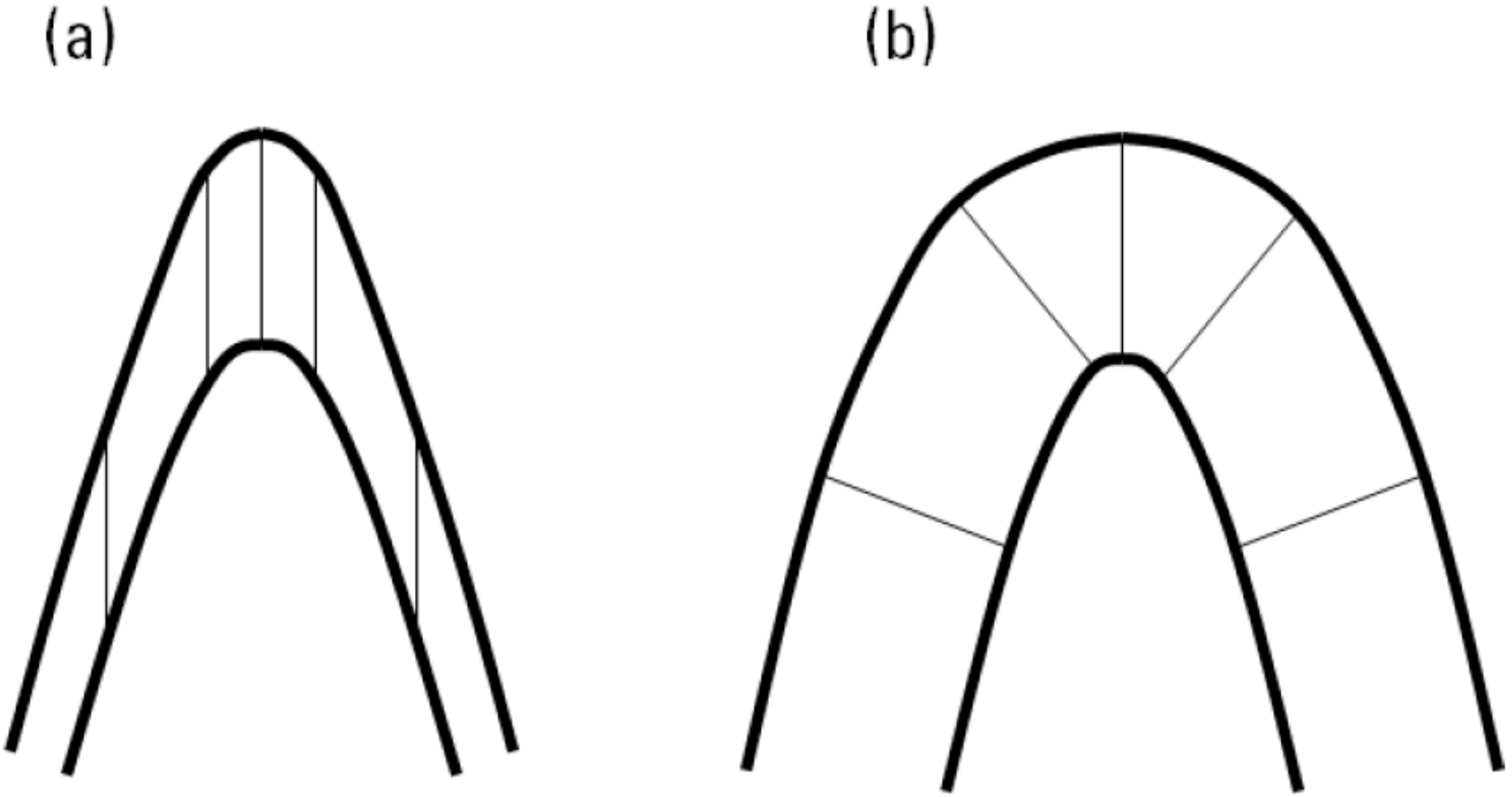

Figure 5. The geometry of (a) similar fold and (b) parallel fold. Modified from Ramsay (1967).

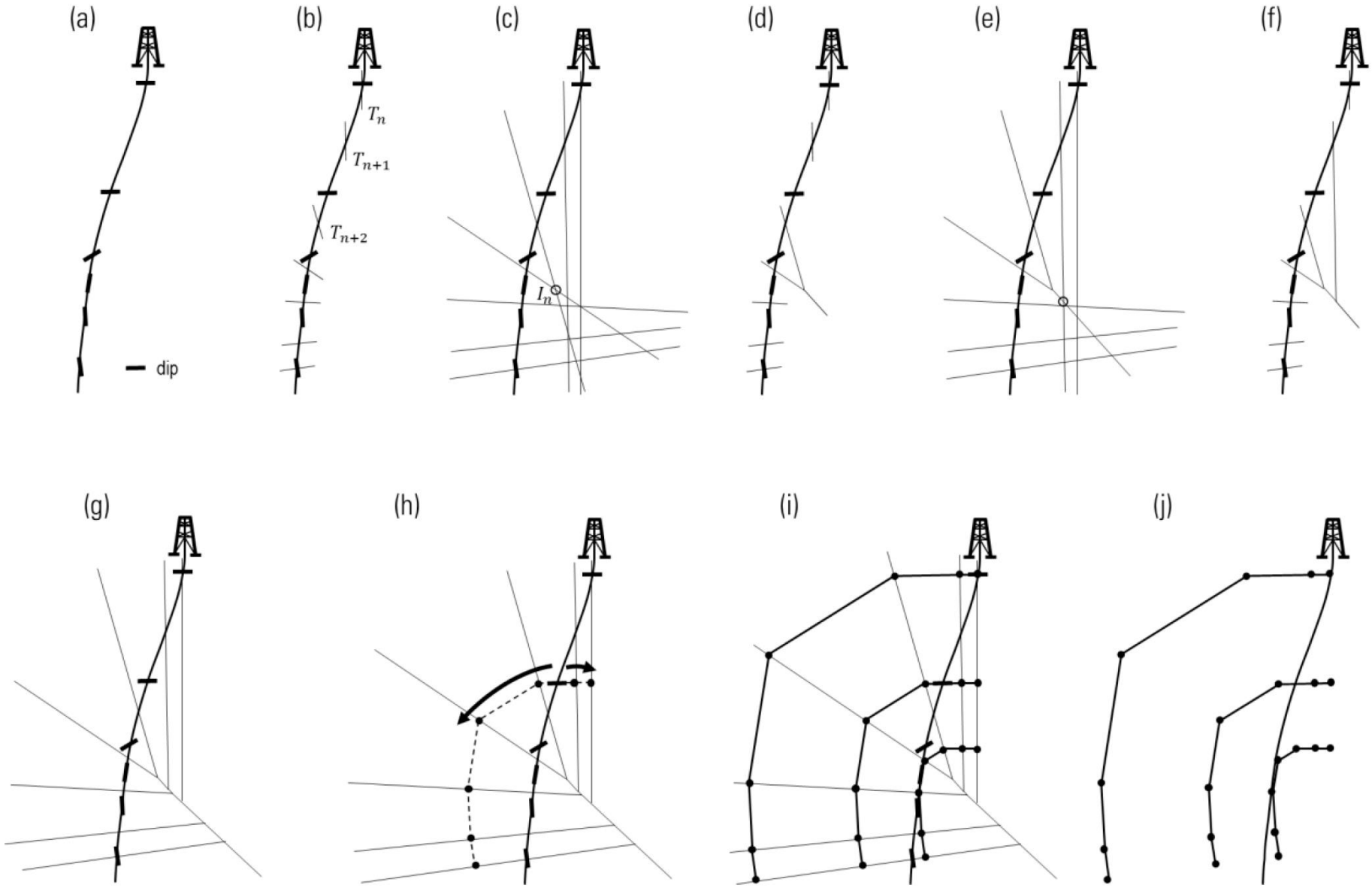

Figure 6. Computation steps of the new parallel model.

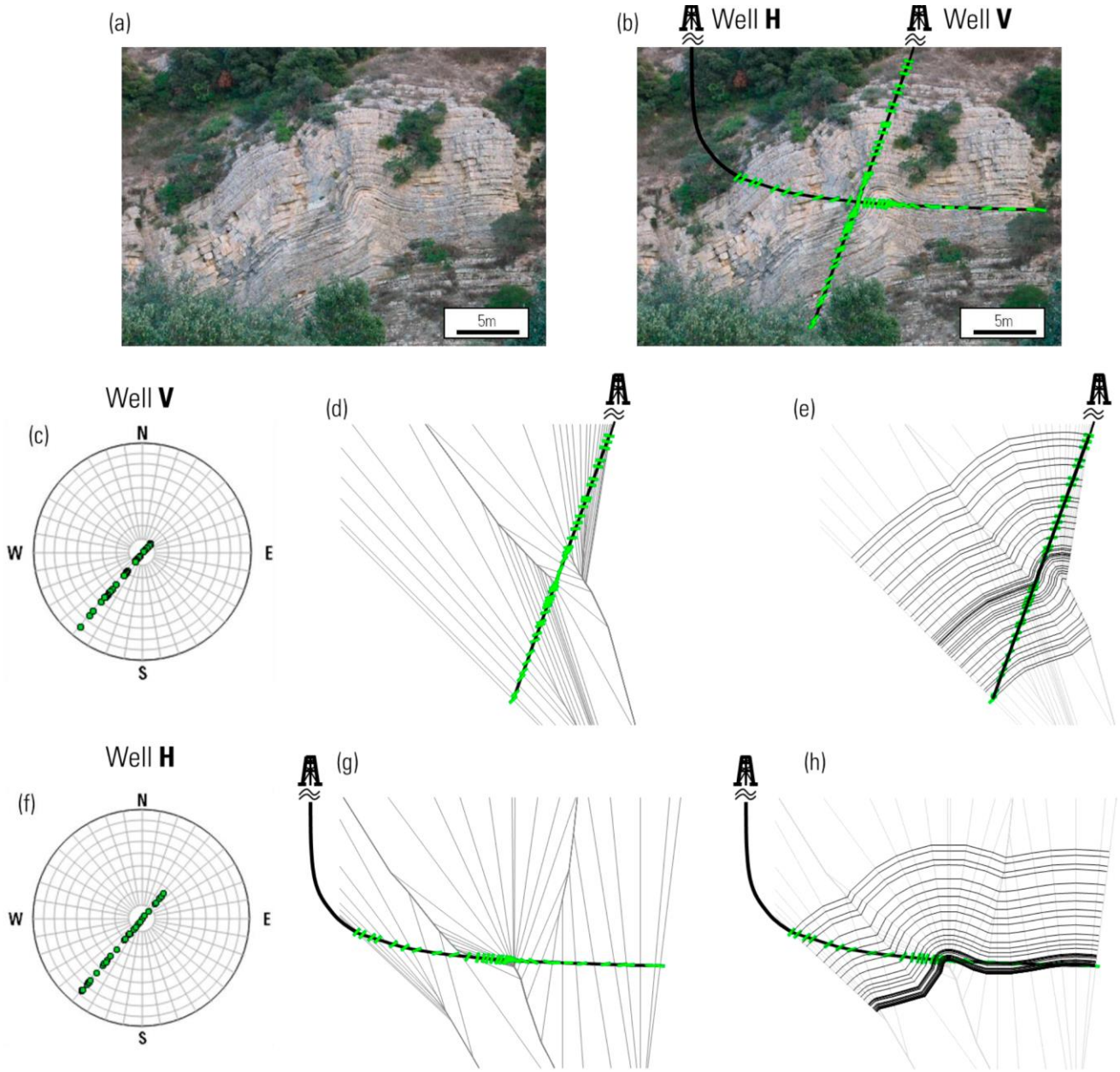

Figure 7. New parallel model applied to the data from imaginary wells: (a) outcrop photograph, (b) two imaginary wells superimposed on the outcrop, (c) stereonet showing the dips from well V (upper hemisphere, Schmidt net), (d) guiding web created with dip from well V, (e) layers created with dip from well V, (f) to (h) are the equivalent of (c) to (e) applied to the dips from well H.

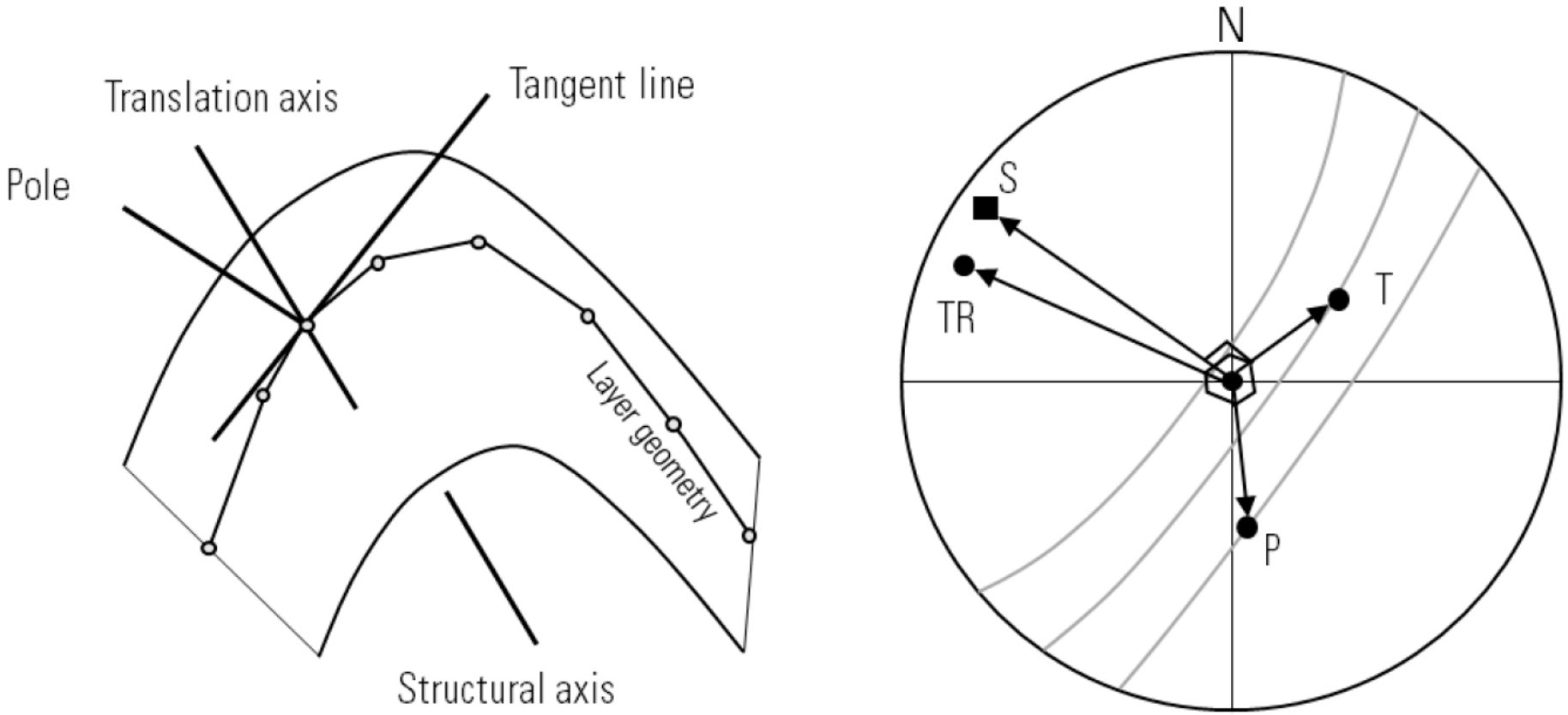

Figure 8. Relationship between axes on the stereonet (upper hemisphere, Schmidt net). Dipping 10° in azimuth 305°. The conicity of the small circle is 75°s. S: structural axis, TR: translation axis, T: tangent line, P: pole.

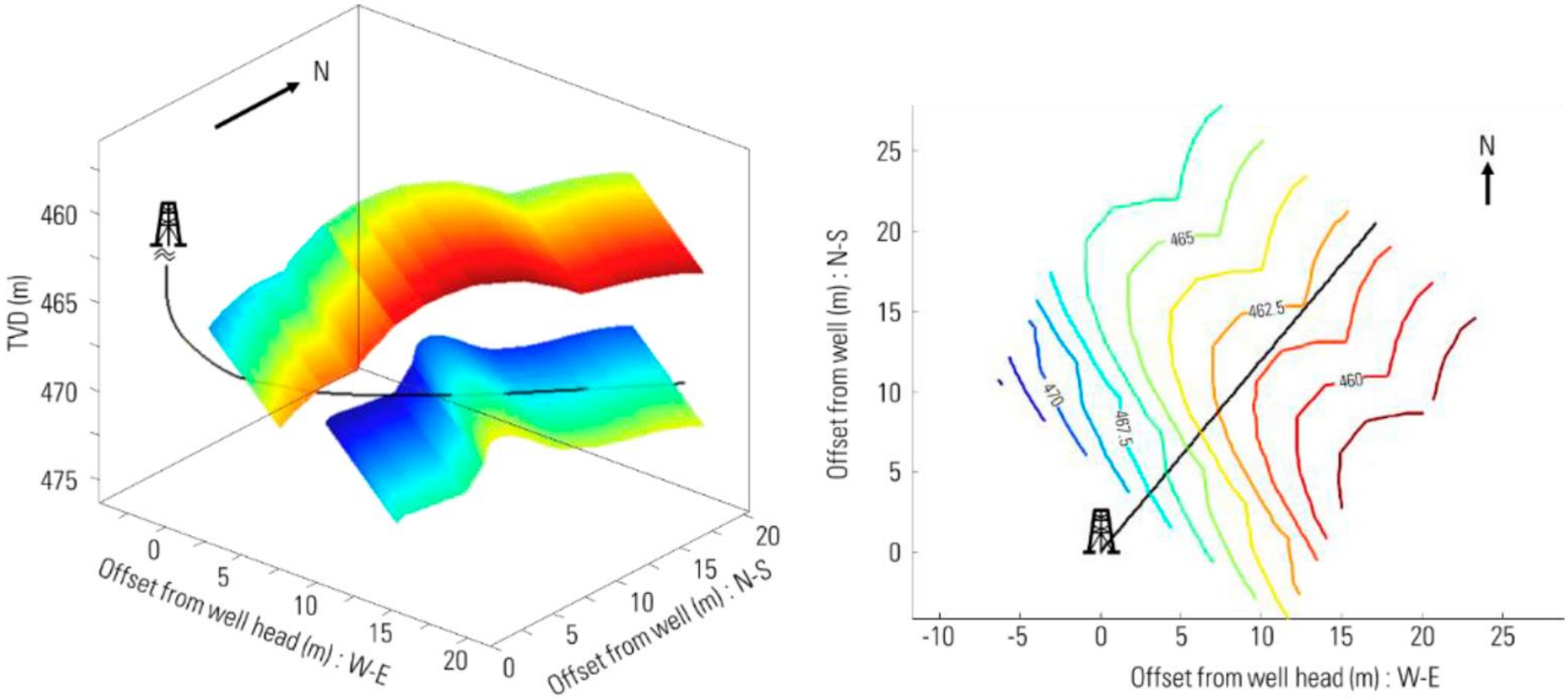

Figure 9. Near-well 3D structure model (left) and the contour map of the top layer in the top view (right). The color shows the true vertical depth; red is shallower and blue is deeper.

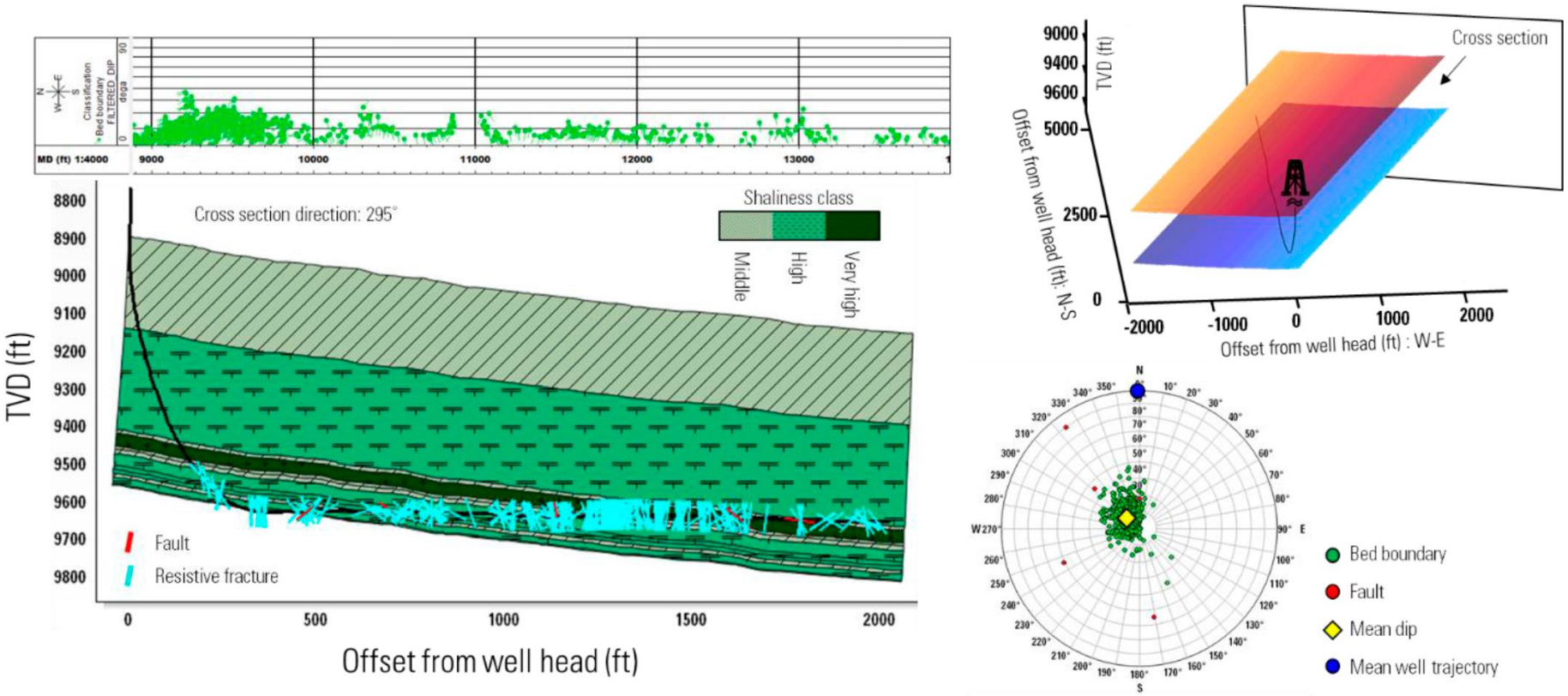

Figure 10. Workflow result with data from a shale formation. The cross section is filled with a discrete log created from gamma ray log (left) and stereonet showing dip and well information (right, upper hemisphere, Schmidt net).

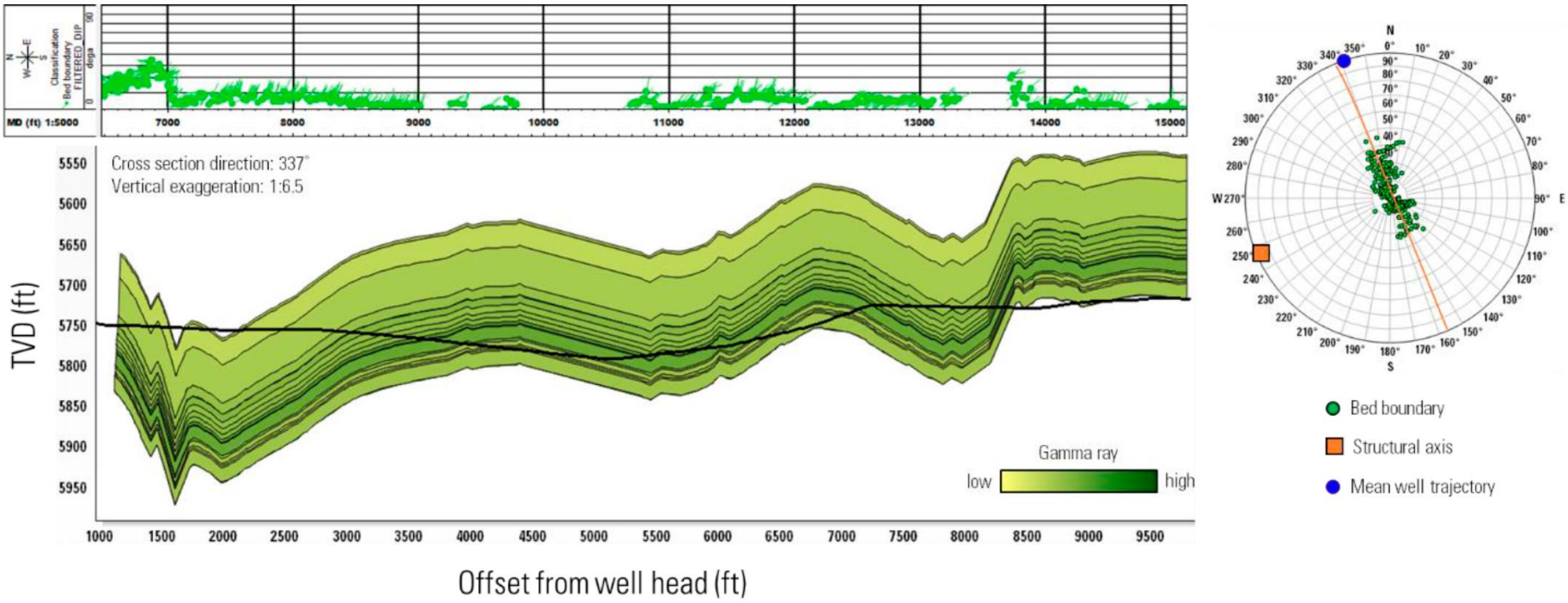

Figure 11. Workflow result with data from the Marcellus Formation. Cross section is filled with gamma ray log (left) and stereonet showing dip and well information (right, upper hemisphere, Schmidt net).